Effect of Ionic Strength on the Conformation of Myosin Subfragment 1–Nucleotide Complexes

Y. Michael Peyser,* Katalin Ajtai,† Thomas P. Burghardt,† and Andras Muhlrad*
*Hebrew University Hadassah School of Dental Medicine, Institute of Dental Sciences, Department of Oral Biology, Jerusalem 91120, Israel and †Department of Biochemistry and Molecular Biology, Mayo Foundation, Rochester, Minnesota 55905 USA

ABSTRACT The effect of ionic strength on the conformation and stability of S1 and S1–nucleotide–phosphate analog complexes in solution was studied. It was found that increasing concentration of KCl enhances the reactivity of Cys^{707} (SH1 thiol) and Lys^{84} (reactive lysyl residue) and the nucleotide-induced tryptophan fluorescence increment. In contrast, high KCl concentration lowers the structural differences between the intermediate states of ATP hydrolysis in the vicinity of Cys^{707}, Trp^{510} and the active site, possibly by increasing the flexibility of the molecule. High concentrations of neutral salts inhibit both the formation and the dissociation of the M**.ADP.Pi analog S1.ADP.Vi complex. High ionic strength profoundly affects the structure of the stable S1.ADP.BeF_x complex, by destabilizing the M*.ATP intermediate, which is the predominant form of the complex at low ionic strength, and shifting the equilibrium to favor the M**.ADP.Pi state. The M*.ATP intermediate is destabilized by perturbation of ionic interactions possibly by disruption of salt bridges. Two salt-bridge pairs, Glu^{501}–Lys^{505} in the Switch II helix and Glu^{776}–Lys^{84} connecting the catalytic domain to the lever arm, seem most appropriate to consider for participating in the ionic strength-induced transition of the open M*.ATP to the closed M**.ADP.Pi state of S1.

INTRODUCTION

Myosin is a motor protein responsible for powering muscle contraction and a large number of motile events in eukaryotic cells. The motor activity of myosin is based on its interaction with actin, which is coupled with hydrolysis of ATP. The myosin head, called subfragment 1 (S1), is where the sites responsible for binding of actin and nucleotide are located. (Myosin sequence numbering is from chicken pectoralis muscle (Maita et al., 1991) except where noted otherwise.) The structure of S1 is highly dynamic and it changes upon interaction with ATP, ADP- and phosphate-analogs and actin. Conformational changes taking place during the consecutive steps of myosin-catalyzed ATP hydrolysis were described by Bagshaw and Trentham (1974).

$$\mathrm{M+ATP} \overset{1}{\leftrightarrow} \mathrm{M^*.ATP} \overset{2}{\leftrightarrow} \mathrm{M^{**}.ADP.Pi} \overset{3}{\leftrightarrow} \mathrm{M^*.ADP+Pi} \overset{4}{\leftrightarrow} \mathrm{M+ADP+Pi}$$

SCHEME 1

M, M*.ATP, M**.ADP.Pi, and M*.ADP are intermediate states of ATP hydrolysis, having distinct spectral properties and representing different conformations (Werber et al., 1972). The conformational changes occurring during the transitions between the intermediate states of ATP hydrolysis are the source of force generation. Thus the description of the conformation of myosin in the intermediate states is essential for the understanding of the motor mechanism. Structural analogs of phosphate (Pi)—vanadate (Vi), beryllium fluoride (BeF_x) and aluminum fluoride (AlF_4^-) complexes—were found to substitute Pi and stop the myosin-catalyzed ATP hydrolysis by forming stable "trapped" complexes with myosin and ADP (Goodno, 1979; Maruta et al., 1993; Phan and Reisler, 1992; Werber et al., 1992). The complexes of the recombinant truncated Dictyostelium S1 (S1dC) with BeF_x, AlF_4^-, and Vi—S1dC.ADP.BeF_x, S1dC.ADP.AlF_4^-, S1dC.ADP.Vi—were crystallized, and their atomic structure solved (Fisher et al., 1995; Smith and Rayment, 1996). The structure of these complexes was significantly different and indicated that S1dC.ADP.BeF_x resembles the M*.ATP, whereas S1dC.ADP.AlF_4^- and S1dC.ADP.Vi mimic the M**ADP.Pi intermediate state. However, it was shown recently that the atomic structures of the crystallized smooth myosin S1 in complex with ADP.AlF_4^- and ADP.BeF_x are practically identical and closely resemble those of S1dC.ADP.AlF_4^-, and S1dC.ADP.Vi (Dominguez et al., 1998). Very recently, scallop myosin S1 complexed with ADP was crystallized in a third conformation (Houdusse et al., 1999), which was believed to be another ATP state of the molecule. Biochemical studies of the relationship of the S1.ADP.PA complexes to the states of ATP hydrolysis were carried out also on rabbit skeletal muscle S1 in solution. The findings of these studies, including those of near-ultraviolet (UV) CD measurements (Peyser et al., 1997), kinetics of modification of Cys^{707} (Phan et al., 1997) and Lys^{84} (Ajtai et al., 1999), mostly supported the conclusions of the results obtained with the recombinant truncated Dictyostelium S1 (Fisher et

Received for publication 1 March 2001 and in final form 9 May 2001.

Address reprint requests to Thomas P. Burghardt, Mayo Clinic and Fndn., Dept. of Biochem./Molec. Biol., Guggenheim 16, Rochester, MN 55905-0002. Tel.: 507-284-8120; Fax: 507-284-9349; E-mail: burghardt@mayo.edu.

Abbreviations used: S1, myosin subfragment 1; ATPγS, adenosine-5′-*O*-3-thiotriphosphate; AlF_4^-, aluminum fluoride complex; BeF_x, beryllium fluoride complex; CD, circular dichroism; CPM, 7-diethylamino-3-(4′-dimaleimidylphenyl)-4-methyl coumarin; HEPES, 4-(2-hydroxyethyl)-1-piperazine ethane sulfonic acid; NMR, nuclear magnetic resonance; PA, phosphate analog; Pi, phosphate; SH1, most reactive thiol or Cys707; S1dC, truncated Dictyostelium S1; TNBS, 2,4,6-trinitrobenzene sulfonate; TNP-, trinitrophenyl-; UV, ultra violet; Vi, vanadate.

0006-3495/01/08/1101/14 $2.00

al., 1995; Smith and Rayment, 1996), i.e., S1.ADP.BeF_x resembled the M*.ATP whereas S1.ADP.AlF_4^- and S1.ADP.Vi mimicked the M**.ADP.Pi intermediate state. However, beside similarities, differences were also found in the solution studies between the structure of the PA-containing complexes and that of the intermediate states of the ATP hydrolysis.

Because of the inconsistent results about the resemblance of S1.ADP.BeF_x complex to the intermediates of the ATPase cycle, it seemed to us of interest to study why this complex mimics the M*.ATP state in Dictyostelium and rabbit S1, and the M**.ADP.Pi state in smooth muscle S1. The conflicting results may derive from differences between S1's obtained from various sources or from the different conditions used for crystallization and solution studies. The first possibility seems improbable in the light of a recent preliminary communication where a crystal structure of truncated *Dictyostelium* S1.ADP.BeF_x complex resembling the M**.ADP.Pi state was obtained (Holmes, 1998). ^{19}F NMR spectroscopy suggested that ADP.BeF_x, trapped S1 in 0.18 M KCl, exists in more than one conformer, perhaps mimicking both M*.ATP and M**.ADP.Pi (Henry et al., 1993). If so, the various S1 crystals might select one of the ADP.BeF_x conformers mimicking either the M* or the M** state, depending on which conformer is the predominant form under the given conditions. A factor that may affect the distribution between the two conformers is ionic strength, because the crystals of smooth muscle S1.ADP.BeF_x were grown at high ionic strength (1.8 M ammonium sulfate) (Dominguez et al., 1998) and those of Dictyostelium S1.ADP.BeF_x in a moderate ionic-strength medium in the presence of polyethylene glycol (Fisher et al., 1995).

Because we found in preliminary studies (Peyser et al., 1999) that the resemblance of S1.ADP.BeF_x to transient conformations occurring during ATP hydrolysis is ionic-strength-dependent, we decided to generalize the investigation to the effect of ionic strength on the structure, formation, and dissociation of various S1–nucleotide complexes. We studied the effect of ionic strength on the conformation of rabbit skeletal S1 complexed with various nucleotides and phosphate analogs in solution. Several methods were used, including the measurement of rates of modification of Cys^{707} (SH1 thiol) and Lys^{84} (reactive lysine residue), rate of dissociation of the stable S1.ADP.Vi complex, tryptophan fluorescence intensity increment and near-UV CD spectra. High ionic strength was found to influence the conformation of the S1 complexes and to shift the equilibrium of the S1.ADP.BeF_x conformers from predominantly resembling M*.ATP to predominantly resembling M**.ADP.Pi. We studied why the increasing ionic strength abolishes the M* intermediate structure in favor of a structure most closely resembling the M** intermediate. Because higher ionic strength weakens salt bridges, the possibility was considered that the stability of the induced M* conformation is due to formation of salt bridges that are broken during the structural transition from M* to M** accompanying ATP hydrolysis. We have identified possible salt bridges participating in this proposed process by comparing the available crystal structures of the M* and M** intermediates.

MATERIALS AND METHODS

Chemicals

ATP, ADP, TNBS, $BeCl_2$ (dissolved in 1% HCl), α-chymotrypsin, dithioerythritol, HEPES, phenylmethane sulfonyl fluoride, and TrisHCl were from Sigma (St. Louis, MO). ATPγS was purchased from Boehringer Mannheim (Indianapolis, IN). The ADP contamination of the ATPγS is less than 5% according to polyethyleneimine cellulose thin layer chromatography. CPM was from Molecular Probes (Eugene, OR). All other chemicals were reagent grade. A stock solution of sodium vanadate (100 mM) was prepared according to Goodno (1979). Sodium fluoride stock solutions were prepared on the day they were used.

Preparation of proteins

Myosin was prepared from back and leg muscles of rabbit by the method of Tonomura et al. (1966). S1 was obtained by digestion of myosin filaments with α-chymotrypsin as described by Weeds and Taylor (1975). Protein concentrations were obtained by absorbance, using an A(1%) at 280 nm of 5.5, and 7.5 for myosin and S1, respectively. Molecular masses were assumed to be 500 and 115 kDa for myosin and S1, respectively.

Formation of stable S1.ADP.phosphate analog complexes (trap formation)

S1 (17–30 μM) was incubated in 10 mM or 500 mM KCl, 1 mM $MgCl_2$, and 30 mM HEPES, pH 7.0 at 25°C with 0.2 mM ADP for 5 min. In the case of BeF_x, or AlF_4^- containing complexes, 5 mM NaF was also present. After that time, 0.2 mM of Vi, $BeCl_2$, or $AlCl_3$ was added, and the incubation continued at 25°C for 20 min. When studying the formation of the "trapped" S1.ADP.Vi complex, aliquots were taken at given time intervals after addition of Vi to assay K^+-(EDTA)-activated ATPase activity.

K^+-(EDTA)-activated ATPase assay

This was assessed from the inorganic phosphate produced, measured by malachite green assay according to Kodama et al. (1986). The reaction was performed at 25°C on 0.5 mL aliquots taken at various time intervals. Incubation times were chosen so that no more than 15% of the ATP was hydrolyzed. The assay contained 1 μM S1, 2 mM ATP, 6 mM EDTA, 600 mM KCl, and 50 mM Tris-HCl buffer, pH 8.0.

Decomposition of the stable S1.MgADP.Vi complex

This was followed essentially according to Peyser et al. (1996) by EDTA chase. The metal ions, which have been dissociated from the S1.MgADP.Vi complex, are chelated with EDTA that reacts only with free Me^{2+} but not with Me^{2+} trapped in the complex. The EDTA-chelated Me^{2+} cannot reenter the complex, which decomposes in the absence of divalent cation. The S1.MgADP.Vi complex was incubated at 25°C in the presence of 4 mM EDTA and the decomposition of the complex was

followed by measuring the recovery of the K^+-(EDTA)-activated ATPase activity as described above.

Kinetics of S1 modification

The time course of trinitrophenylation of Lys^{84} was spectrophotometrically followed essentially as described earlier (Muhlrad and Takashi, 1981). TNBS (final concentration 100 μM) was added to 10 μM S1 in the presence or absence of nucleotides in 1 mM $MgCl_2$, 30 mM TrisHCl, pH 7.8, and either 10 mM KCl or 500 mM KCl. The reaction was performed in the absence or presence of nucleotides (0.2 mM ADP, 6 mM ATP, 0.2 mM ATPγS) bound to the active site or after active site trapping with MgADP and Vi, BeF_x, or AlF_4^-. The reaction was carried out in a thermostated cell of a Unikon 810P spectrophotometer (Zurich, Switzerland) at 25°C. The absorbance change at 345 nm was recorded and the number of TNP groups introduced was calculated. The reaction of S1 with the TNBS has fast and slow components (Kubo et al., 1960). In the fast reaction, the trinitrophenylation of Lys^{84} and the rest of S1 lysines takes place, whereas, in the slow reaction, only the rest of the S1 lysines are modified. Under the conditions of the measurements, trinitrophenylation of Lys^{84} is essentially finished during the first 10–20 min of the reaction. Initial velocity of the modification of the slowly reacting lysines, v_2, was calculated from the reaction rate at 30 min after addition of TNBS by accounting for changes in TNBS and unmodified lysine concentrations during the first 30 min of the reaction. Initial velocity of trinitrophenylation of Lys^{84} (v_1) was obtained by subtracting v_2 from the initial velocity of the overall process (v). Because the modification of Lys^{84} is a pseudo first-order reaction under the conditions of the experiment (10-fold molar excess of TNBS over S1), the first-order rate constants could be calculated from v_1.

The time course of the reaction of Cys^{707} (SH1) with CPM was followed as described recently (Phan et al., 1997) by monitoring the fluorescence change accompanying the modification at 20°C in a thermostated cell holder of a PTI Spectrofluorometer at excitation and emission wavelengths of 390 and 475 nm, respectively. In these measurements, 0.5 μM CPM was added to 5 μM S1 in the presence or absence of nucleotides (nucleotide concentration as during trinitrophenylation, except ATP, which was 0.5 mM) and 30 mM HEPES, 1 mM $MgCl_2$, pH 7.0, and either 10 or 500 mM KCl. A 10-fold molar excess of S1 over CPM was used in the experiment to limit the reaction to 10% of the protein population. This limits the modification to the highly reactive SH1 thiol and excludes the reaction with SH2 (Phan et al., 1997). Under these conditions, both in the presence and absence of nucleotides and phosphate analogs, the reaction of SH1 with CPM can be described by a single exponential from which the rates of SH1 modifications were calculated.

Circular dichroism

Near-UV CD spectra were recorded on a JASCO J715 spectropolarimeter (Tokyo, Japan) as described earlier (Peyser et al., 1997). Protein spectra measurements were carried out in a 1-cm thermostated cell at 20°C containing 20 μM S1, 30 mM HEPES at pH 7. The buffer also contained various concentrations of KCl to alter ionic strength. In addition, some samples contained nucleotides and phosphate analogs as described in Kinetics of S1 modification. In samples containing ATP, an ATP-regenerating system (5 μM pyruvate kinase and 5 mM phosphoenolpyruvate) was added to keep the ATP concentration constant. To obtain a spectrum, CD was recorded from a sample containing the S1 complex, and, subtracted from this was a similarly recorded spectrum from an identical sample except without protein. The CD spectra are expressed as extinction, $\Delta\varepsilon$ $(M\ cm)^{-1}$,

$$\Delta\varepsilon = \frac{\theta}{32980\ Cl} \qquad (1)$$

where θ is mdeg, l is the optical path length in cm, C is the molar concentration of S1.

Nucleotide-induced tryptophan fluorescence increment

Tryptophan fluorescence of 1 μM S1 in 30 mM HEPES, 1 mM $MgCl_2$, pH 7.0 and either 10 or 500 mM KCl was recorded at 20°C before (F_0) and after (F) addition of nucleotides and phosphate analogs (for concentrations, see Kinetics of S1 modification except for ATP, which was 0.5 mM) in a thermostated cell of a PTI spectrofluorometer. Excitation and emission were set at 297 and 332 nm, respectively. The fluorescence intensity increments induced by nucleotides and phosphate analogs were expressed as percent of fluorescence increment, $(F - F_0)\ 100/F_0$.

Decomposition of heterogeneous S1 conformations into elementary forms

We compared the CD spectrum from S1+ATP to that from S1, S1.ATPγS, S1.ADP.AlF_4^-, and S1.ADP to estimate the fractional contributions from the ATPase intermediates, M, M*.ATP,M**, and M*.ADP, as described previously (Peyser et al., 1997).

The S1.ADP.BeF_x conformation was decomposed into contributions from the M*.ATP and M** transient intermediate conformations using the formula,

$$E(\text{S1.ADP.BeF}_x) = a_1 E(\text{S1.ATP}\gamma\text{S}) + a_2 E(\text{S1.ADP.PA}), \qquad (2)$$

where E is a signal derived from a variety of sources described below, a_1 and a_2 are the fractional concentrations for the M*.ATP and M** conformations, and PA is AlF_4^- or Vi. In addition to Eq. 2, we always require $a_1 \geq 0$, $a_2 \geq 0$, and $a_1 + a_2 \leq 1$. With Eq. 2, we presume that S1.ATPγS and S1.ADP.PA induce pure M*.ATP and M** conformations.

Signals represented by E include the fluorescence increment, the modification rate of Lys^{84}, or the near-UV CD spectrum. Only S1.ADP.AlF_4^- was used to model the M** conformation near-UV CD spectrum because the S1.ADP.Vi spectrum contains contributions from the bound Vi (Ajtai et al., 1998). The fluorescence increment and modification rate signals provide single constraints on unknowns a_1 and a_2, and, consequently, cannot determine both coefficients independently. In these cases, we assume $a_2 = 1 - a_1$, i.e., that the S1.ADP.BeF_x conformation is faithfully described by a mixture limited to the conformations induced by S1.ATPγS and S1.ADP.PA. CD spectra signals provide multiple constraints (one at each point in the observed wavelength domain) for unknowns a_1 and a_2 such that these unknowns may be determined independently by least squares. If the sum $a_1 + a_2 < 1$, the remainder $1 - (a_1 + a_2)$ is that part of the distribution of conformations in S1.ADP.BeF_x that cannot be modeled with S1.ATPγS or S1.ADP.AlF_4^-. We found, in all cases tested, that $a_1 + a_2 = 1$, suggesting a mixture limited to the conformations induced by S1.ATPγS and S1.ADP.PA, faithfully describes the distribution of conformations in S1.ADP.BeF_x.

Effect of neutral salts on protein structure

The presence of small charged atoms or molecules in the buffer weakens the accessible ionic interactions within myosin by interposing themselves between the interacting groups. Accordingly, we consider the possibility that increasing ionic strength weakens salt bridges in the myosin that stabilize the M*.ATP conformation in S1.ADP.BeF_x. Different neutral salts are also known to promote or destabilize hydrophobic interactions in proteins according to the Hoffmeister/Von Hippel series (Von Hippel and

Wong, 1964; Creighton, 1993; Green, 1932). Consequently, we must also consider the possibility that increasing ionic strength affects hydrophobic interactions in the myosin. We investigated the nature of the ionic strength effect on S1 by observing how it differs for various neutral salts in the Hoffmeister/Von Hippel series. The ions from the neutral salt bind to S1 according to

$$T + A \rightleftharpoons B$$

SCHEME 2

where T is a free-ion binding site on S1, A is the ion, and B is the occupied ion-binding site. The concentration of binding sites is a constant, $[N] = [T] + [B]$, where [ ] implies concentration. At equilibrium, if p is the fraction of occupied sites,

$$p = \frac{[A]/\Gamma}{1 + [A]/\Gamma} \tag{3}$$

where $\Gamma = [T]_{eq}[A]_{eq}/[B]_{eq}$ is the equilibrium constant. A signal, F, sensitive to protein conformation, depends on ionic strength by

$$F([A]) = F(0) - \{F(0) - \alpha\}p$$

$$= \alpha + \frac{F(0) - \alpha}{1 + [A]/\Gamma} \tag{4}$$

where α is the signal level unaffected by ion binding. If Γ or $F(0) - \alpha$ are affected by the stability of the hydrophobic interactions in S1, then they will be systematically perturbed by the neutral salts in the Hoffmeister/Von Hippel series.

Identification of salt bridges in the M* and M** complexes

Potential salt bridges were identified by measuring distances between side-chain oxygen atoms in the negatively charged residues glutamate (OE1 or 2) or aspartate (OD1 or 2) and the side-chain nitrogen atoms in the positively charged residues lysine (NZ), arginine (NH1 or 2), or histidine (ND1 or NE2). For our purposes, oppositely charged atoms from these residues that are separated by <5 Å qualify as a salt bridge. This criterion was applied to myosin S1 crystal structures from Dictyostelium discoideum (S1dC) and smooth muscle (SmS1). Crystal structures representing the myosin M* intermediate are MgADP.BeF_x trapped (Fisher et al., 1995) or MgATPγS bound (Gulick and Rayment, 1997) S1dC. Crystal structures representing the M** intermediate are MgADP.AlF_4^- (Fisher et al., 1995) or MgADP.Vi trapped (Smith and Rayment, 1996) S1dC. To identify potential salt bridges in the M** intermediate corresponding to residues in the lever arm that are not in the S1dC structures, we consulted the crystal structure of MgADP.AlF_4^--trapped SmS1 (Dominguez et al., 1998).

RESULTS

Trinitrophenylation of Lys[84]

Lys^{84} is the most reactive lysine residue of the myosin head (Kubo et al., 1960) located in the 27-kDa N-terminal segment of the molecule (Mornet et al., 1980; Hozumi and Muhlrad, 1981) at an interface of the catalytic and lever arm domains (Ajtai et al., 1999). TNBS preferentially trinitrophenylates Lys^{84}. The rate of reaction of Lys^{84} with TNBS is three orders of magnitude faster than the rest of the lysine residues of S1 (Muhlrad and Takashi, 1981). The trinitrophenylation of S1 takes place in two phases. The rapid first phase of the reaction is from modification of both Lys^{84} and the other lysines of S1 (Muhlrad and Takashi, 1981; Tonomura et al., 1963). This is followed by a slower second phase after completion of Lys^{84} trinitrophenylation when only the other lysines of S1 are reacting. The modification of Lys^{84}, but not the rest of lysine residues of S1, is strongly inhibited by ATP and ATP analogs (Tonomura et al., 1963; Muhlrad and Fabian, 1970).

TABLE 1 Pseudo first-order rate constants for trinitrophenylation of Lys^{84} in S1 in the absence and presence of nucleotides and phosphate analogs

	Rate constant ± SE × 10^5 (sec^{-1}) or inhibition in %*			
Addition to S1	10 mM KCl		500 mM KCl	
none	524 ± 11.3	0	682 ± 9.9	0
ADP	261 ± 9.1	51	326 ± 10.5	53
ATPγS	265 ± 15.9	50	517 ± 10.9	24
ADP.BeF_x	211 ± 9.7	60	147 ± 1.6	79
ATP	134 ± 2.4	75	154 ± 3.3	78
ADP.AlF_4^-	120 ± 2.3	78	172 ± 4.1	75
ADP.Vi	129 ± 3.1	76	147 ± 16.2	79

*Mean ± SE of six independent experiments.
Experimental conditions are discussed in Materials and Methods.

We followed the kinetics of S1 trinitrophenylation in the absence of nucleotide; in the presence of ATP, ADP, and ATPγS; and trapped with ADP.BeF_x, ADP.AlF_4^-, and ADP.Vi in the presence of TrisHCl buffer, pH 7.8, and either 10 or 500 mM KCl. The pseudo first-order rate constants for modification of Lys^{84} were calculated from the time courses of each reaction (see Materials and Methods) and are shown in Table 1. At low ionic strength, all ligands strongly inhibited the rate of trinitrophenylation of Lys^{84} without affecting the rate of modification of other lysine residues. On the basis of the extent of inhibition, the ligands are classified into two groups. ADP, ATPγS, and ADP.BeF_x belong to the first group with 51–60%, and ATP, ADP.AlF_4^- and ADP.Vi to the second group with 75–78% inhibition, all in agreement with our previous results (Ajtai et al., 1999). In the presence of MgATP, S1 predominantly populates the M**.ADP.Pi state of the ATPase cycle (Bagshaw and Trentham, 1974). Because ADP.AlF_4^- and ADP.Vi behave like ATP regarding the inhibition of Lys^{84} modification, it follows that the structure of S1.ADP.AlF_4^- and S1.ADP.Vi complexes in the vicinity of Lys^{84} resemble the structure of the M**.ADP.Pi state. The results indicate that, under the conditions of the experiment, the structure of S1.ADP.BeF_x in the vicinity of Lys^{84} is similar to the structure of S1.ATPγS. Thus, like S1.ATPγS (Goody and Hofmann, 1980), S1.ADP.BeF_x resembles the structure of M*.ATP. Addition of 500 mM KCl increases the rate of the reaction in the presence of each ligand, except with ADP.BeF_x, where the rate of trinitrophenylation decreases and approaches the rate observed in the presence of ATP,

TABLE 2 Effect of ionic strength on the rate constants of alkylation with CPM of Cys^{707} in S1 and nucleotide–S1 complexes

	Rate constant ± SE 10^3 (sec^{-1})*	
Addition to S1	10 mM KCl	500 mM KCl
None	9.1 ± 0.77	18.2 ± 1.62
ADP	13.0 ± 0.952	21.7 ± 1.86
ATPγS	13.9 ± 1.06	22.7 ± 2.04
ADP.BeF_x	11.3 ± 0.99	21.1 ± 1.94
ATP	8.7 ± 0.76	15.5 ± 1.37
ADP.Vi	8.3 ± 0.72	19.2 ± 1.78

*Mean ± SE of five independent experiments.
Experimental conditions are discussed in Materials and Methods.

TABLE 3 Effect of ionic strength on the nucleotide-induced tryptophan fluorescence increment in S1

	Fluorescence increment* (%)	
Addition to S1	10 mM KCl	500 mM KCl
ADP	5.8 ± 0.1	12.4 ± 0.2
ATPγS	9.1 ± 0.4	17.4 ± 1.5
ADP.BeF_x	14.0 ± 0.6	24.5 ± 0.3
ATP	25.1 ± 0.8	27.2 ± 0.2
ADP.AlF_4^-	26.6 ± 0.4	26.4 ± 0.3

*Mean ± SE of four independent measurements.
Experimental conditions are discussed in Materials and Methods.

ADP.AlF_4^-, and ADP.Vi (75–79% inhibition). This shows that, at high ionic strength, the structure of S1.ADP.BeF_x in the vicinity of Lys^{84} resembles that of the M**.ADP.Pi state.

Alkylation of Cys^{707} (SH1) by CPM

The kinetics of Cys^{707} modification with CPM was followed by fluorescence increase, which can be described by a single exponential when the reaction was carried out in the presence of 10-fold molar excess of S1 over the reagent. The modification was performed in the presence and absence of nucleotides and phosphate analogs and the apparent first-order rate constants determined as described previously (Phan et al., 1997) (Table 2). When the reaction was carried out at low ionic strength, the rate of the reaction was low in the presence of ATP and ADP.Vi, i.e., in cases where S1 is in the M**.ADP.Pi state, and in the absence of nucleotides. The reaction was fast in the presence of ATPγS, i.e., in the M*.ATP state, and with ADP, whereas, with ADP.BeFx, intermediate velocity was obtained, which was nearer to the rate observed with ATPγS than to the rate with ATP. These results are in accordance with those obtained in an earlier study (Phan et al., 1997). At high ionic strength, the rate of reaction became much faster in all cases. The velocity at high ionic strength decreased in the order ATPγS > ADP > ADP.BeFx > ADP.Vi > no nucleotide > ATP but the measured reaction rate differences between the various cases became significantly smaller than the differences obtained in the presence of low ionic strength buffer.

Nucleotide-induced tryptophan fluorescence increment

Addition of ATP or ADP to S1 causes a significant increase in tryptophan fluorescence intensity (Werber et al., 1972). ATP induces about a 25% increment, but increments induced by ADP or ATPγS (Goody and Hofmann, 1980) are much smaller. According to recent studies (Johnson et al., 1991; Batra and Manstein, 1999; Onishi et al., 2000; Park and Burghardt, 2000; Yengo et al., 2000) Trp^{510} is the nucleotide-sensitive tryptophan in S1. We studied the tryptophan fluorescence increment induced by addition of ADP and phosphate analogs to S1 (Werber et al., 1992) and found that ADP.AlF_4^- causes about the same increment as ATP, but the increase induced by ADP.BeF_x was considerably smaller. In this work, we studied the effect of high KCl concentration on the tryptophan fluorescence of S1 and compared the tryptophan fluorescence increment caused by the addition of nucleotides and PAs at high and low ionic strength. Tryptophan fluorescence of S1 was reduced only by 3–4% in the absence of nucleotides at high ionic strength, which may reflect to a weak quenching effect of high KCl concentration (data not shown). The effect of ionic strength on the nucleotide-induced fluorescence increment was more significant (Table 3). At low ionic strength, the highest increment was obtained by ADP.AlF_4^-, which was closely followed by ATP. The lowest increments were observed with ADP and ATPγS, whereas the ADP.BeF_x increment was intermediate but closer to ATPγS than to ATP. The results indicate that ADP.AlF_4^- mimics the M**.ADP.Pi state but that ADP.BeF_x probably exist in two conformer forms, one mimicking the M**.ADP.Pi and the other the M*.ATP state with the equilibrium favoring the latter. At high ionic strength, the fluorescence increments induced by all nucleotides except ADP.AlF_4^- became significantly higher and the contrast among the different states significantly smaller. The tryptophan fluorescence in the presence of ADP.BeF_x at high ionic strength is nearer to that observed with ATP or ADP.AlF_4^- than with ATPγS. This suggests that, at high ionic strength, the equilibrium between the two ADP.BeF_x conformers is shifted to the direction of the M**.ADP.Pi form.

Effect of ionic strength on the near-UV CD spectrum of S1 in the presence of nucleotides and PAs

The near-UV CD spectrum of S1 between 250 and 310 nm is dominated by contributions from the aromatic amino acid residues. The 255–270-, 270–275-, 275–285-, and 285–

310-nm regions are generated by Phe, Tyr, Tyr, and Trp together, and Trp chromophores, respectively (Strickland, 1974). We found recently that addition of nucleotides and PAs significantly affect the near-UV CD spectrum of S1 at low ionic strength (Peyser et al., 1997), likely through the nucleotide-sensitive tryptophan Trp^{510} (Park et al., 1996) and possibly through the interaction of the adenine ring of the nucleotides with the aromatic Tyr^{135} and Trp^{131} residues in the active site of S1 (Strickland, 1974). The various nucleotides and PAs differently affect the near-UV CD spectrum of S1 and characterize the intermediate conformations of S1 during ATPase.

The near-UV CD of S1+MgATP is a sum of spectra from the transient intermediates M*.ATP, M**.ADP.Pi, and M*.ADP with weights corresponding to their fractional concentrations. These intermediates are modeled by the analog conformations S1.ATPγS or S1.ADP.BeF_x, S1.ADP.AlF_4^-, and S1.ADP, respectively, from which we computed the fractional concentrations with a method described previously (Peyser et al., 1997). The fractional occupation of the transient intermediates observed with CD agrees with earlier results from time resolved experiments (Bagshaw and Trentham, 1974) indicating M** accounts for >80% of the transient population. We also found that, at low ionic strength, the S1.ADP.BeF_x and S1.ATPγS spectra are very similar, both mimicking the M*.ATP intermediate.

In this work, we studied the influence of nucleotides and PAs on the near-UV CD spectrum of S1 at high ionic strength (Fig. 1). All the nucleotides and PAs affected the spectrum, however, the contrast among their effects diminishes with increasing ionic strength. Nevertheless, the calculated fractional concentrations of the transient intermediate states in S1+MgATP indicated the M**.ADP.Pi state is predominant, accounting for 61% of the total population, with the remainder in M*.ATP. In this calculation, M*.ATP and M**.ADP.Pi are modeled with S1.ATPγS and S1.ADP.AlF_4^-, respectively. If S1.ADP.BeF_x replaces S1.ATPγS as the model for M*.ATP, the M**.ADP.Pi and M*.ATP states account for 52 and 46% of the population with the remainder in the M*.ADP state. The predominance of the M**.ADP.Pi state, at >80% at low ionic strength, diminishes to ~60% at high ionic strength. This may be an accurate representation of the state distribution during ATPase or caused by the lower contrast among the analog CD spectra leading to ambiguous assignments of distribution coefficients.

Finally, expanding the S1+MgATP spectrum in terms of the analog spectra from S1.ATPγS, S1.ADP.BeF_x, and S1.ADP, all at high ionic strength, produces fractional concentrations of 33, 67, and 0% of the total population. The latter results, obtained using S1.ADP.BeF_x to replace S1.ADP.AlF_4^- in the analysis of S1+MgATP, hints that S1.ADP.BeF_x is an M**.ADP.Pi analog in these conditions. We tested the heterogeneity of the near-UV CD spectrum from S1.ADP.BeF_x as a function of ionic strength using Eq. 2. The CD results at 500 mM KCl are computed from the spectra in Fig. 1, spectra at other ionic strengths are not shown. These CD results are summarized in Table 4, where we show that, for increasing ionic strength, S1.ADP.BeF_x changes from a predominantly M*.ATP to a predominantly M**.ADP.Pi analog. In contrast, if we perform a similar test on the S1.ATPγS analog, where, in Eq. 2, we reverse the roles of S1.ADP.BeF_x and S1.ATPγS, we find $a_2 = 0$ for all signals, implying that S1.ATPγS has no overlap with the pure M**.ADP.Pi analog regardless of ionic strength.

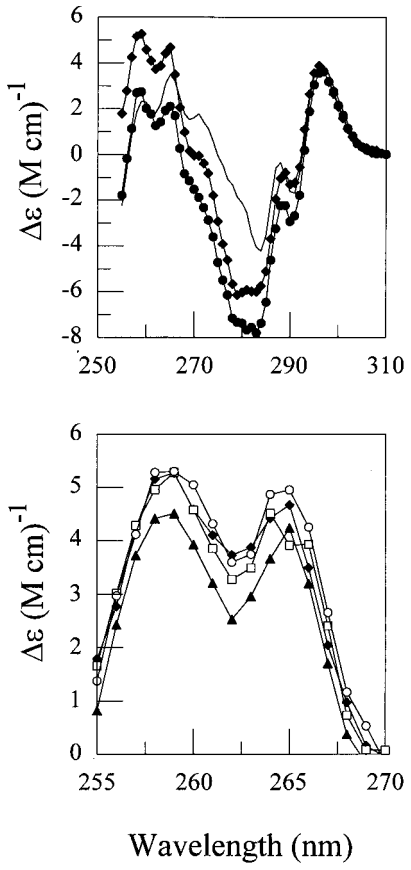

FIGURE 1 Near-UV CD spectra of S1 and S1-nucleotide complexes in the presence of 500 mM KCl. *Top*: S1 (—), S1.ADP (●), and S1.ADP.BeF_x (◆). *Bottom*: S1.ATPγS (▲), S1.ADP.BeF_x (◆), S1.ADP.AlF_4^- (○), and S1+ATP (□). Top and bottom panels have differing wavelength domains. Spectra from the trapped nucleotide analogs and S1+ATP collected in the bottom panel are essentially indistinguishable over wavelengths 270 nm ≤ λ ≤ 310 nm. Experimental conditions are described in Materials and Methods.

Heterogeneity of the S1.ADP.BeF_x conformation

We tested the heterogeneity of the S1.ADP.BeF_x conformation as a function of ionic strength with Eq. 2 using the fluorescence increment and the modification rate of Lys84 as the signal sources (data from Tables 1 and 3). The results,

TABLE 4 Heterogeneity of the ADP.BeF$_x$ analog as a function of ionic strength*

KCl (mM)	Signal†	% M*.ATP	% M**
10	trinitrophenylation	63	37
	ΔF	72	28
	CD	87	13
60	CD	35	65
100	CD	17	83
500	trinitrophenylation	0	100
	ΔF	21	79
	CD	14	86

*Experimental error for the fractional concentrations is ≤10%.
†Trinitrophenylation is TNBS modification of Lys^{84}. $\Delta F \equiv 100(F - F_0)/F_0$ where F is the analog trapped or nucleotide bound, and F_0 is substrate free, S1 tryptophan fluorescence. CD is the near-UV CD spectrum.

tabulated in Table 4, closely follow those indicated by the near-UV CD spectrum of S1.ADP.BeF$_x$.

Effect of ionic strength on the formation and dissociation of the stable S1.MgADP.Vi complex

The formation of the "trapped" S1.MgADP.Vi complex is accompanied by the loss of ATPase activity that recovers with dissociation of the complex (Goodno, 1979). Thus, we conveniently monitored formation and dissociation of the complex by measuring K^+(EDTA)-activated ATPase. Formation of the S1.MgADP.Vi complex was achieved by adding vanadate to S1 in the presence of saturating concentrations of ADP and $MgCl_2$ at various ionic strengths. Under these conditions, the formation of the complex can be described by the scheme (Werber et al., 1992),

$$\text{S1.MgADP} + \text{Vi} \underset{k_{-1}}{\overset{k_1}{\longleftrightarrow}} \text{S1.MgADP.Vi} \underset{k_2}{\overset{k_2}{\leftrightarrow}} \text{S1}^{\#}.MgADP.Vi.$$

SCHEME 3

The first step is assumed to be a rapid binding equilibrium that is followed by a slow isomerization step. S1$^{\#}$ indicates an altered conformation. The ionic strength during the formation reaction was defined by increasing concentrations of KCl or K-acetate (Fig. 2, *A* and *B*, respectively). The time course of ATPase disappearance in each case was fitted to a single exponential and characterized by a first-order kinetic constant, k_{obs}. The obtained k_{obs} values are plotted in Fig. 3. Ionic strength higher than 200 or 350 mM strongly inhibited the formation of the S1.MgADP.Vi complex with KCl and K-acetate, respectively.

According to Scheme 3, and because the first step is always at equilibrium with constant $K_1 = k_1/k_{-1}$, k_{obs} is, in general, a function of K_1 and the forward and backward rates of isomerization, k_2 and k_{-2}. The stability of the vanadate-trapped S1 (see below) is such that k_{-2} may be neglected and k_{obs} depends on K_1 and k_2 alone. Whether ionic strength affects K_1 and k_2 was investigated using the dependence of k_{obs} on vanadate concentration, [Vi] (Fig. 4). The k_{obs} versus [Vi] curves at two KCl concentrations were fitted with hyperbolas from which k_2 (k_{obs} for [Vi] $\rightarrow \infty$) and K_1 ([Vi] at which $k_{obs} = \frac{1}{2}k_2$) values were calculated. At 10 or 500 mM KCl, k_2 is 1.91 or 0.26 sec^{-1}, and K_1 is 0.18 or 0.14 mM, respectively. The results show that k_2 is very dependent, whereas K_1 is comparatively independent of KCl concentration. Thus, ionic strength dramatically affects the slow isomerization step in Scheme 3 but not the transient binding of the PA.

We also studied the effect of the ionic strength of the spontaneous dissociation of the S1.MgADP.Vi complex by EDTA chase as described in Materials and Methods. The time course of the dissociation of S1.MgADP.Vi in the presence of various concentrations of KCl or K-acetate was followed by monitoring the recovery of the K^+(EDTA)-activated ATPase activity and presented in Fig. 5, *A* and *B*. Increasing concentrations of KCl and K-acetate strongly inhibited the rate of the ATPase recovery, i.e., the dissociation of the complex. The inhibition of the ATPase recovery is not due to denaturation of S1 during the long incubation at 20°C at high salt concentration because addition of actin causes the fast dissociation of the complex (Werber et al., 1992) and the full recovery of ATPase activity (results not shown). Thus the results indicate that the increasing ionic strength significantly enhances the stability of the S1.MgADP.Vi complex and, therefore, that of the M**.ADP.Pi state.

Effect of Hoffmeister/Von Hippel series neutral salts on the stability of the M**.ADP.Pi conformation

We observed the effect of ionic strength on the rate of formation of the S1.MgADP.Vi complex for various neutral salts in the Hoffmeister/Von Hippel series (Von Hippel and Wong, 1964; Green, 1932). As before, the time course of ATPase disappearance accompanying stable trap formation was fitted to a single exponential and characterized by a first-order kinetic constant, k_{obs}. The neutral salts investigated, listed in decreasing order for their ability to stabilize hydrophobic interactions in proteins, were K-acetate, NaCl, KCl, KBr, KI, and KSCN. Available data suggests that NaCl and KCl may be equivalent perturbants (Von Hippel and Wong, 1964) of hydrophobic interactions in proteins, whereas other data suggests that KCl is the more potent perturbant (Green, 1932). The k_{obs} versus salt concentration for K-acetate (■) and KCl (□) are shown in Fig. 3.

The effect of salt concentration on k_{obs} is described by Eq. 4 with the two parameters Γ, and $k_{obs}(0) - \alpha$, corresponding to the ion binding constant and the ion-binding sensitive part of the rate of ATPase change. In Fig. 6, we summarize the values of these parameters computed from the data in Fig. 3 and that from the other ions in the

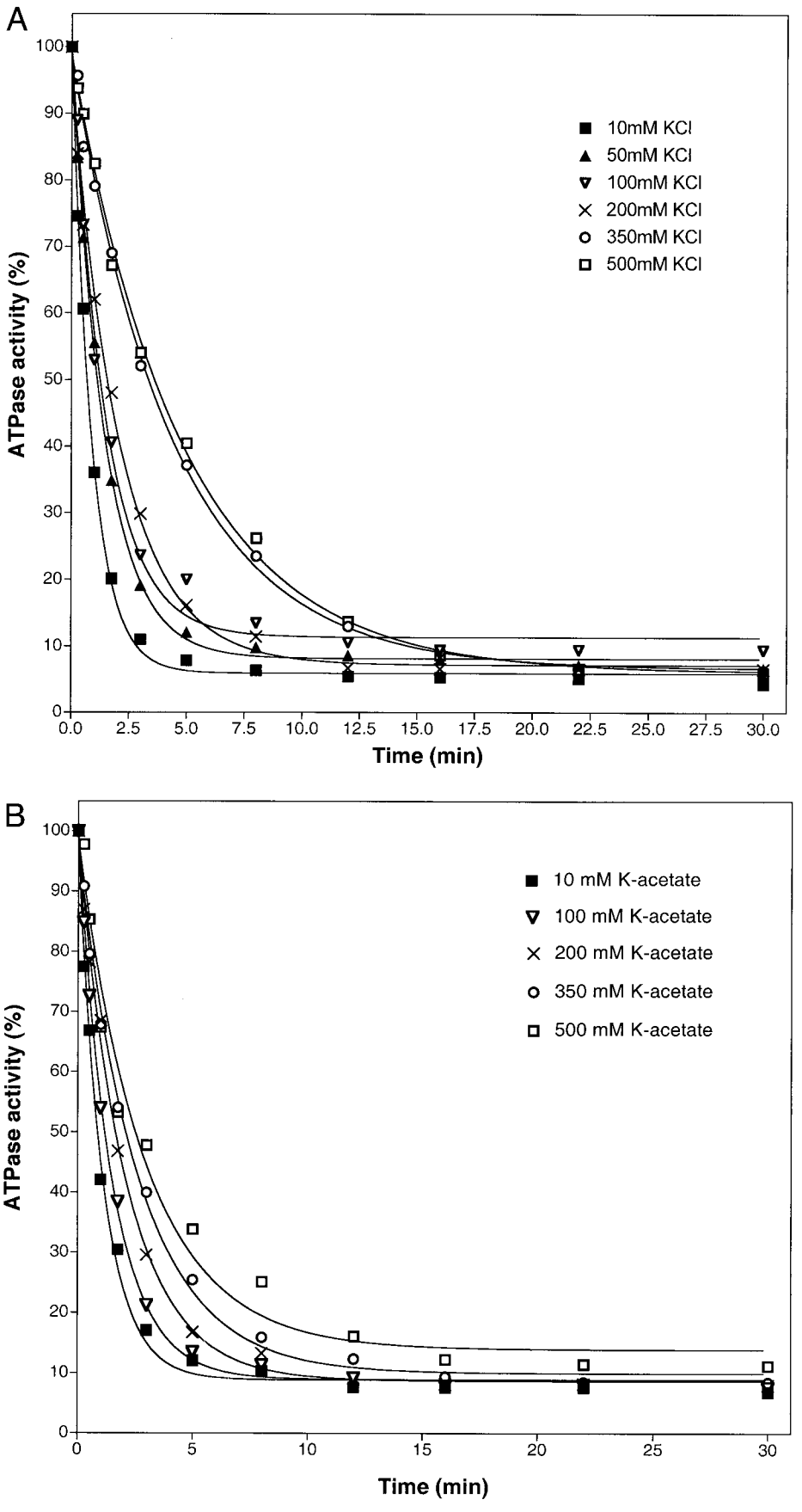

FIGURE 2 The time course of K^+(EDTA)-activated ATPase disappearance during vanadate trapping. Effect of (*A*) KCl or (*B*) K-acetate concentration on trap formation. For details of trap formation and ATPase measurement see Materials and Methods.

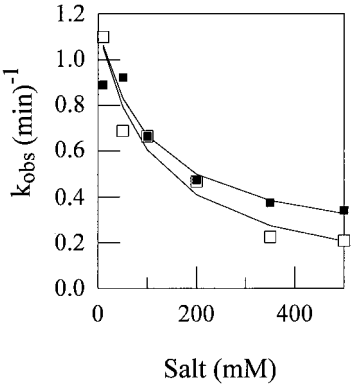

FIGURE 3 The observed rate of K^+-EDTA ATPase inhibition due to vanadate trapping of S1 versus concentration of the neutral salts K-acetate (■) and KCl (□). Solid lines indicate a fitted curve derived from Eq. 4 where k_{obs} replaces $F([A])$ at salt concentration $[A]$. The fitted parameters for these curves are plotted in Fig. 6.

Hoffmeister/Von Hippel series. Figure 6 shows that ion-dependent parameters have no obvious dependence on the order of the Hoffmeister/Von Hippel series salts, suggesting that the S1 ionic strength effect pertains to electrostatic rather than hydrophobic interactions in the protein. This ionic strength effect, characteristic to S1 during the "salting-in" phase of its solubility, depends on the concentration but not the nature of the neutral salt. The "salting-out" effect, known to depend on the position of the neutral salt in the Hoffmeister/Von Hippel series, apparently begins to be relevant only at higher salt concentrations (Green, 1932).

Involvement of salt bridges in the stabilization of the M*.ATP state

We found in this study that, in the S1.ADP.BeF_x complex, the M*.ATP conformation is destabilized at high ionic strength in favor of the M**.ADP.Pi conformation. Our results using the neutral salts from the Hoffmeister/Von Hippel series suggests that this phenomenon originates from the disruption of ionic, rather than hydrophobic, interactions in the protein. Salt bridges are an important component of the ionic stabilization energy in a protein and their disruption at high ionic strength might be responsible for the lower stability of the M*.ATP conformation in these conditions. We searched for possible candidate salt bridges stabilizing M*.ATP in the available crystal structures of S1.

We began our search by identifying all oppositely charged side-chain atoms from salt bridge-forming residues separated by <5 Å. This criterion identifies about 100 potential salt bridges in S1 in each structure investigated. We narrowed the field by making additional assumptions about the properties anticipated for M*.ATP stabilizing bridges. First, we assume that the salt bridges of interest are not present in the M** intermediate, suggesting that we can ignore any bridge common to both the M*.ATP and M**.ADP.Pi conformations. Second, we assume that the salt bridges of interest are necessary to stabilize M*.ATP such that they must appear in any structural representation of M*.ATP. By the second assumption, we ignore salt bridges unique to M*.ATP that do not appear in both the MgADP.BeF_x trapped and MgATPγS bound S1dC structures.

Given the above, we identified the 10 intradomain salt bridges (numbering from S1dC) Asp^{21}–Arg^{7}, Glu^{99}–Arg^{44}, Glu^{150}–Arg^{147}, Glu^{187}–Arg^{131}, Glu^{395}–Lys^{391}, Glu^{492}–Lys^{496}, Asp^{509}–Lys^{557}, Asp^{718}–Lys^{721}, Asp^{724}–Lys^{728}, Glu^{755}–Arg^{704}, and the three interdomain bridges Asp^{614}–Lys^{435}, Glu^{755}–Lys^{84}, Glu^{756}–Arg^{33}. Intradomain salt bridges link residues within one of the three domains designated as catalytic, converter, and lever arm (Geeves and Holmes, 1999). Interdomain salt bridges link together any two of these domains. The interdomain salt bridges identified link the converter and catalytic domains (Asp^{614}–Lys^{435}) or the lever arm and catalytic domains (Glu^{755}–Lys^{84} and Glu^{756}–Arg^{33}).

We further narrow the field by requiring that the residues engaged in a potential salt bridge are conserved between S1dC and chicken skeletal S1 but allowing interchangeability between Glu and Asp and among Lys, Arg, and His. This restriction leaves us with a set of five possibilities: Glu^{150}–Arg^{147} (near-active site), Glu^{492}–Lys^{496} (Switch II helix), Asp^{718}–Lys^{721} (converter domain), Glu^{755}–Arg^{704} (lever arm), and Glu^{755}–Lys^{84} (lever arm to catalytic). The location of two of these salt bridge pairs makes them remarkable relative to the other pairs in the set. The Glu^{492}–Lys^{496} pair is located in the Switch II helix, at the heart of the energy transduction mechanism. The Switch II helix deforms during the M*.ATP to M**.ADP.Pi transition causing a 5-Å displacement of the closest charged atoms in side chains from Glu^{492} and Lys^{496} (from 3.7 to 8.8 Å). The Glu^{755}–Lys^{84} pair spans the catalytic and lever arm domains. Lys^{84} is the reactive lysine residue that, when modified, alters the rate of ATP hydrolysis (Fabian and Muhlrad, 1968). Lever arm swinging in the M*.ATP to M**.ADP.Pi transition causes a 23-Å displacement of the closest charged atoms in side chains from Glu^{755} and Lys^{84} (from 3.8 to 27.4 Å, M**.ADP.Pi separation distance taken from SmS1 (Dominguez et al., 1998)). With chicken pectoralis myosin sequence numbering, the salt bridge in the Switch II helix is Glu^{501}–Lys^{505} and the interdomain pair is Glu^{776}–Lys^{84}.

DISCUSSION

In this work, the effect of ionic strength on the structure of S1 complexed with various nucleotides and PAs was studied. It was found that the increase of ionic strength, achieved by increasing concentration of KCl, enhances the accessibility of Cys^{707} and Lys^{84} residues to modifications essentially in all S1-nucleotide complexes. Because Cys^{707}

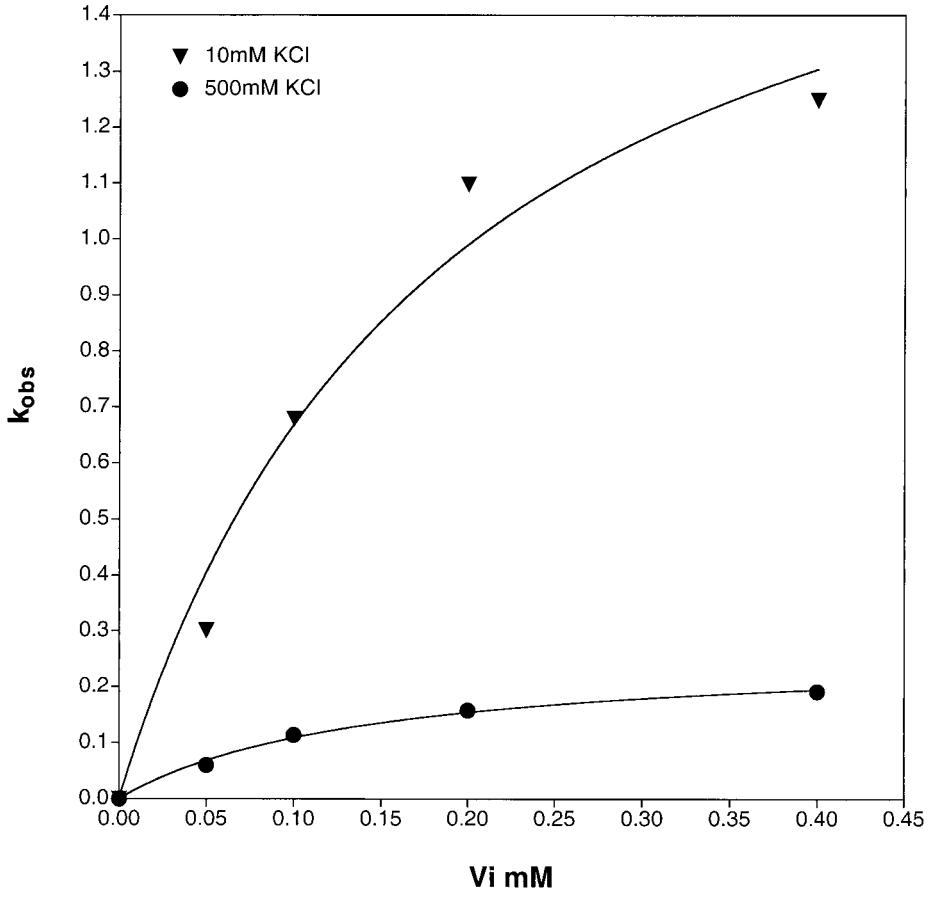

FIGURE 4 Vanadate concentration dependence of the rate constant of S1.ADP.Vi complex formation, k_{obs}, for two KCl concentrations.

and Lys[84] are located at different regions of S1, this effect suggests increased flexibility in the molecular structure with increasing ionic strength.

In addition to the enhanced mobility of the molecule, we found that the structure of the various states of the ATPase cycle, represented by S1-nucleotide complexes, become more similar at high ionic strength. This is manifested in the similar rates of modification of Cys[707] with CPM, in smaller contrast among the near-UV CD spectra for the M*.ATP and M**.ADP.Pi conformations, and in the more uniform fluorescence increment upon nucleotide binding to, or nucleotide analog trapping of, S1. The changes in the near-UV CD spectrum possibly reflects altered local structure at the nucleotide-sensitive tryptophan, Trp[510], and in the active site where the adenine ring of the nucleotide interacts with local aromatic residues. Thus, the active site and the vicinity of Cys[707] and Trp[510] may become less sensitive to the differences among the states of the ATPase cycle at high ionic strength. Alternatively, the contrast among the rates of trinitrophenylation of Lys[84] for the various nucleotide–S1 complexes is about the same at low and high ionic strength, indicating that the similarity of the S1 ATPase intermediates does not carry over to the vicinity of Lys[84].

The increase in ionic strength significantly enhances the nucleotide-induced tryptophan fluorescence increment with all nucleotides and PAs used in this study (except AlF_4^-), but it only slightly reduces tryptophan fluorescence in the absence of nucleotides (data not shown). Chymotryptic S1 has five Trps and it is believed that essentially only the fluorescence of Trp[510] (Johnson et al., 1991; Batra and Manstein, 1999; Onishi et al., 2000; Park and Burghardt, 2000; Yengo et al., 2000) is affected by nucleotides. The slight decrease in the fluorescence of S1 tryptophans in the absence of nucleotides may indicate a weak quenching by high concentration of KCl, but the enhanced nucleotide-induced fluorescence increment at high ionic strength points to the moving of Trp[510] to a more protected environment.

The results of the present work are in accordance with former studies showing that, at low ionic strength, S1.ADP.BeF_x resembles the M*.ATP but S1.ADP.AlF_4^- and S1.ADP.Vi complexes mimic the M**.ADP.Pi states (Fisher et al., 1995; Peyser et al., 1997; Phan et al., 1997; Ajtai et al., 1999). The comparison of the rates of modification of Lys[84], the tryptophan fluorescence enhancement increment, and the near-UV CD spectra of S1.ADP.BeF_x to that obtained from S1 in the M**.ADP.Pi and M*.ATP

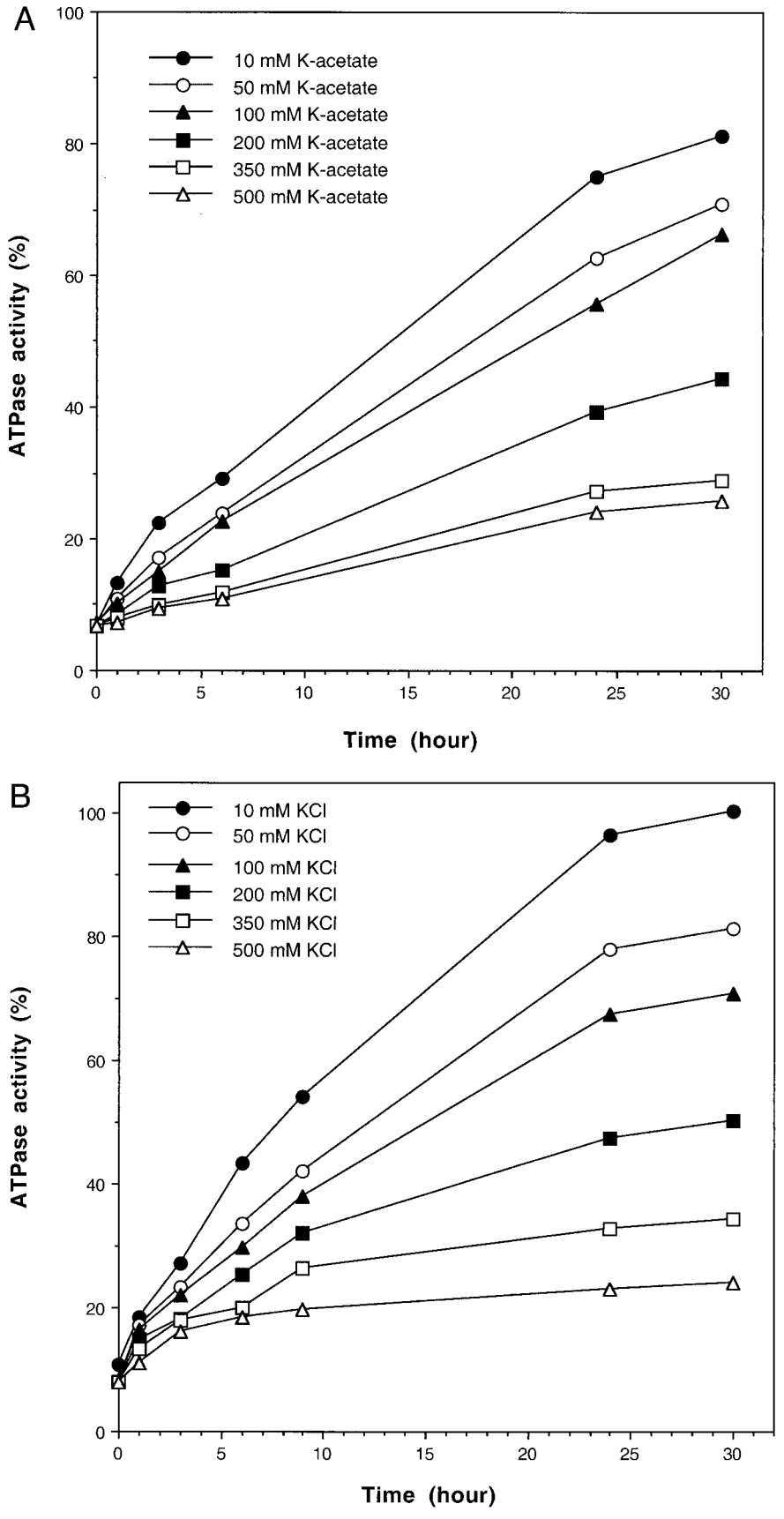

FIGURE 5 Effect of (*A*) K-acetate or (*B*) KCl concentration on the dissociation of the Vi from the S1.MgADP.Vi complex by EDTA chase.

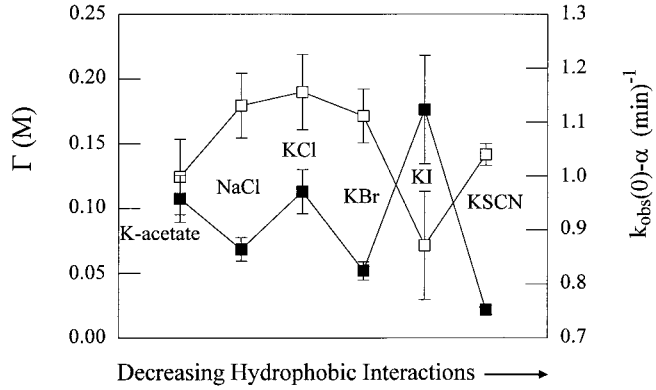

FIGURE 6 Fitted parameters Γ (■), and $\{k_{obs}(0) - \alpha\}$ (□), corresponding to the ion-binding constant and the ion-binding sensitive part of the rate of ATPase change for ions in the Hoffmeister/Von Hippel series. The data used to find Γ and $k_{obs}(0) - \alpha$ for K-acetate and KCl are shown in Fig. 3. NaCl and KCl may occupy identical positions on the x-axis (Von Hippel and Wong, 1964).

states show that the S1.ADP.BeF_x structure more closely resembles that of M*.ATP at low ionic strength. At high ionic strength, these same indicators of protein structure show that the S1.ADP.BeF_x structure more closely resembles that of M**.ADP.Pi. On the basis of these results we propose that S1.ADP.BeF_x at equilibrium exists in two forms, one mimicking M*.ATP, the other M**.ADP.Pi. This equilibrium is affected by ionic strength, in the manner suggested by the variation in the fractional distribution of the S1.ADP.BeF_x between the M*.ATP and M**.ADP.Pi conformers tabulated in Table 4. As such, low ionic strength favors M*.ATP and high ionic strength the M**.ADP.Pi form.

Our finding that, at high ionic strength, the M**.ADP.Pi state is favored over the M*.ATP state is probably due to the decreased stability of the latter state, which is supported by the results of Johnson and Taylor (1978) who showed that the M*.ATP to M**.ADP.Pi transition is accelerated at high ionic strength. The shifting equilibrium from M*.ATP to M**.ADP.Pi at higher salt concentration may explain the apparent inconsistency of the crystallographic studies, i.e., the observation that the atomic structure of S1.ADP.BeF_x crystals grown at moderate ionic strength mimic M*.ATP (Fisher et al., 1995) whereas those grown at high ionic strength resemble the M**.ADP.Pi form (Dominguez et al., 1998). Ions bind to S1 with a binding constant of ~80 mM (Table 4 or Fig. 6) shifting the M*⇌M** equilibrium in skeletal S1.ADP.BeF_x. The crystallization of S1dC.ADP.BeF_x produces the M* conformation at moderate salt concentrations (170 mM) where the predominant conformation, based on the skeletal data, is expected to be firmly on the M** side of the equilibrium. This apparent discrepancy suggests that the S1dC.ADP.BeF_x complex binds salt with lower affinity than the skeletal S1.ADP.BeF_x complex. The salt-binding constants for these complexes may differ due to experimental conditions (for instance polyethylene glycol is present during crystallization of S1dC.ADP.BeF_x) or to more interesting structural differences, including lever arm length.

Neutral salt concentration alters S1.ADP.BeF_x conformation through its effect on ionic and hydrophobic interactions stabilizing the protein structure. The small charged atoms or molecules from the neutral salt in the buffer suppress the accessible ionic interactions within myosin by interposing themselves between the interacting groups. Accordingly, there is the possibility that increasing neutral salt concentration weakens salt bridges in the myosin that stabilize the M*.ATP conformation of S1.ADP.BeF_x. Alternatively, neutral salts are also known to systematically affect hydrophobic interactions according to the Hoffmeister/Von Hippel series. Figure 6 indicates the effect of several neutral salts in the Hoffmeister/Von Hippel series on the formation of the S1.ADP.Vi complex. Each neutral salt affects the formation rate of the stable complex in a concentration-dependent manner. However, they behave rather similarly to each other and show no apparent correlation with the Hoffmeister/Von Hippel series. On this basis, we conclude that increasing neutral salt concentration mainly affects S1.ADP.BeF_x conformation by weakening the ionic interactions in the protein structure.

If the dissolution of ionic interactions in S1.ADP.BeF_x causes movement of the predominant equilibrium structure from one like M*.ATP to one like M**.ADP.Pi, solution-exposed salt bridges in S1 might provide the energy-stabilizing M*.ATP at low ionic strength. We inspected and compared crystal structures for the M*.ATP and M**.ADP.Pi intermediates to investigate this possibility. The comparison yielded several pairs of residues potentially forming salt bridges in M*.ATP that dissolve when S1 assumes the M**.ADP.Pi conformation. The residue pairs fall into two classes that form links: within the catalytic, lever arm, or converter domains (intradomain), or, between any two of these three domains (interdomain). Inspection of any of the intradomain salt bridges suggests that they work to stabilize or rigidify domain structure. The interdomain salt bridges appear to maintain relationships among the domains characteristic to the structural intermediate.

We identified two salt bridge pairs, Glu^{501}–Lys^{505} and Glu^{776}–Lys^{84}, that seem most appropriate to consider for participating in the ionic strength-induced M*.ATP to M**.ADP.Pi transition. The Glu^{501}–Lys^{505} intradomain pair is in the Switch II helix responsible for perturbing the ATP-sensitive tryptophan (Trp^{510}) during ATP hydrolysis (Geeves and Holmes, 1999; Onishi et al., 1998). Disturbing the structure of this helix could induce structural changes downstream in the energy transduction pathway, perhaps in the converter domain, that mimic those needed for formation of the M**.ADP.Pi intermediate. The Glu^{776}–Lys^{84} interdomain pair is a good choice for residues to directly stabilize the M*.ATP intermediate due to their location at

the extreme end of the lever arm (headed toward the C-terminus) that can still interact with the catalytic domain. At this point, the least force is needed to maintain a lever arm–catalytic domain relationship characteristic to the M*.ATP conformation. It is not surprising to us that Lys^{84} is involved in this interaction with the lever arm because we have reported in the past on the ability of this residue, when modified with TNP, to alter ATP hydrolysis rates by interfering with lever arm movement (Ajtai et al., 1999).

We found that high ionic strength inhibits the association and dissociation of the stable S1.MgADP.Vi complex mimicking the M**.ADP.Pi state, while other results indicate that high ionic strength destabilizes M*.ATP. These effects, produced by common mechanism, suggests that association and dissociation of the stable S1.ADP.Vi complex depends on the ability of the S1 to maintain an equilibrium between structures that allow or inhibit active site analog association and dissociation. Because increasing ionic strength causes the inhibitory response, we associate it structurally with M**.ADP.Pi, and conclude that it is a conformation closed to substrate binding or release. Low ionic strength promotes free association and dissociation of ADP.Vi with S1 and we associate it structurally with M*.ATP, and conclude that it is a conformation open to substrate binding or release. The "open" and "closed" descriptors are analogous to those used for the M*.ATP and M**.ADP.Pi crystal structures that are based there on the open or closed conformation of the hypothetical "back door" for phosphate release during hydrolysis (Geeves and Holmes, 1999; Yount, 1997). Possibly these similarly characterized phenomena of S1 structure and dynamics are related on a fundamental level. If so, then ATP-driven conformational changes could promote the dissolution of certain salt bridges and the destabilization of M*.ATP. In this scenario, the destabilization of M*.ATP is the initiator of the "open" to "closed" structural transition during energy transduction.

In conclusion, increasing ionic strength significantly affects the structure of S1 and S1–nucleotide complexes. It enhances the reactivity of functional groups, the stability of the M**.ADP.Pi state, and the nucleotide-induced Trp fluorescence increment; and lowers the differences between the structural intermediates of ATP hydrolysis in the vicinity of Cys^{707}, Trp^{510}, and the active site. Increasing ionic strength has a unique effect on the structure of S1.ADP.BeF_x complex, causing the destabilization of the predominant M*.ATP intermediate and shifting the equilibrium to favor M**.ADP.Pi. The mechanism for destabilizing M*.ATP is the dissolution of ionic interactions, possibly specific salt bridges. These ionic interactions appear to be involved in the transition between the open (M*.ATP) and closed (M**.ADP.Pi) forms of the S1.

We thank Susanna P. Garamszegi and Angel Cruz-Walker for making some of the CD measurements and Sungjo Park for helpful discussions.

T.P.B. and K.A. were supported by a grant from the National Institutes of Health (R01 AR39288) and by the Mayo Foundation. A.M. was supported by grant 230/99 from the Israel Science Foundation.

REFERENCES

Ajtai, K., F. Dai, S. Park, C. R. Zayas, Y. M. Peyser, A. Muhlrad, and T. P. Burghardt. 1998. Near UV circular dichroism from biomimetic model compounds define the coordination geometry of vanadate centers in MeVi- and MeADPVi-rabbit myosin subfragment 1 complexes in solution. *Biophys. Chem.* 71:205–220.

Ajtai, K., Y. M. Peyser, S. Park, T. P. Burghardt, and A. Muhlrad. 1999. Trinitrophenylated reactive lysine residue in myosin detects lever arm movement during the consecutive steps of ATP hydrolysis. *Biochemistry.* 38:6428–6440.

Bagshaw, C. R., and D. R. Trentham. 1974. The characterization of myosin-product complexes and product-release steps during the magnesium ion-dependent adenosine triphosphate reaction. *Biochem. J.* 141: 331–349.

Batra, R., and D. J. Manstein. 1999. Functional characterisation of *Dictyostelium* myosin II with conserved tryptophanyl residue 501 mutated to tyrosine. *J. Biol. Chem.* 380:1017–1023.

Creighton, T. E. 1993. Proteins in solution and in membranes. *In* Proteins: Structures and molecular properties. W. H. Freeman, New York. 261–328.

Dominguez, R., Y. Freyzon, K. M. Trybus, and C. Cohen. 1998. Crystal structure of a vertebrate smooth muscle myosin motor domain and its complex with the essential light chain: visualization of the pre-power stroke state. *Cell.* 94:559–571.

Fabian, F., and A. Muhlrad. 1968. Effect of trinitrophenylation on myosin ATPase. *Biochim. Biophys. Acta.* 162:596–603.

Fisher, A. J., C. A. Smith, J. B. Thoden, R. Smith, K. Sutoh, H. M. Holden, and I. Rayment. 1995. X-ray structures of the myosin motor domain of *Dictyostelium discoideum* complexed with MgADP.BeF_x and MgADP-AlF_4. *Biochemistry.* 34:8960–8972.

Geeves, M. A., and K. C. Holmes. 1999. Structural mechanism of muscle contraction. *Annu. Rev. Biochem.* 68:687–728.

Goodno, C. C. 1979. Inhibition of myosin ATPase by vanadate ion. *Proc. Natl. Acad. Sci. U.S.A.* 76:2620–2624.

Goody, R. S., and W. Hofmann. 1980. Stereochemical aspects of the interaction of myosin and actomyosin with nucleotides. *J. Muscle Res. Cell Motil.* 1:101–115.

Green, A. A. 1932. Studies in the physical chemistry of the proteins. *J. Biol. Chem.* 95:47–66.

Gulick, A. M., and I. Rayment. 1997. Structural studies on myosin II: communication between distant protein domains. *BioEssays.* 19: 561–569.

Henry, G. D., S. Maruta, M. Ikebe, and B. D. Sykes. 1993. Observation of multiple myosin subfragment 1-ADP-fluoroberylate complexes by ^{19}F NMR spectroscopy. *Biochemistry.* 32:10451–10456.

Holmes, K. C. 1998. Muscle Contraction. *Novartis Found. Symp.* 213: 76–92.

Houdusse, A., V. N. Kalabokis, D. Himmel, A. G. Szent-Gyorgyi, and C. Cohen. 1999. Atomic structure of scallop myosin subfragment S1 complexed with MgADP: a novel conformation of the myosin head. *Cell.* 97:459–470.

Hozumi, T., and A. Muhlrad. 1981. Reactive lysyl of myosin subfragment 1: location on the 27K fragment and labeling properties. *Biochemistry.* 20:2945–2950.

Johnson, K. A., and E. W. Taylor. 1978. Intermediate states of subfragment 1 and actosubfragment 1 ATPase: reevaluation of the mechanism. *Biochemistry.* 17:3432–3442.

Johnson, W. C., Jr., D. B. Bivin, K. Ue, and M. F. Morales. 1991. A search for protein structural changes accompanying the contractile interaction. *Proc. Natl. Acad. Sci. U.S.A.* 88:9748–9750.

Kodama, T., K. Fukui, and K. Kometani. 1986. The initial phosphate burst in ATP hydrolysis by myosin and subfragment-1 as studied by a mod-

ified malachite green for determination of inorganic phosphate. *J. Biochem.* 99:1465–1472.

Kubo, A., S. Tokura, and Y. Tonomura. 1960. On the active site of myosin A-adenosine triphosphatase. I. Reactivity of the enzyme with trinitrobenzene sulfonate. *J. Biol. Chem.* 235:2835–2839.

Maita, T., E. Yajima, S. Nagata, T. Miyanishi, S. Nakayama, and G. Matsuda. 1991. The primary structure of skeletal muscle myosin heavy chain: IV. Sequence of the rod, and the complete 1,938-residue sequence of the heavy chain. *J. Biochem.* 110:75–87.

Maruta, S., G. D. Henry, B. D. Sykes, and M. Ikebe. 1993. Formation of the stable myosin–ADP–aluminum fluoride and myosin–ADP–beryllium fluoride complexes and their analysis using ^{19}F NMR. *J. Biol. Chem.* 268:7093–7100.

Mornet, D., P. Pantel, R. Bertrand, E. Audemard, and R. Kassab. 1980. Localization of the reactive trinitrophenylated lysyl residue of myosin ATPase site in the NH_2-terminal (27 K domain) pfS1 heavy chain. *FEBS Lett.* 117:183–188.

Muhlrad, A., and F. Fabian. 1970. Effects of substrate and substrate analogues on the trinitrophenylation of myosin. *Biochim. Biophys. Acta.* 216:422–427.

Muhlrad, A., and R. Takashi. 1981. Ionization of reactive lysyl residue of myosin subfragment 1. *Biochemistry.* 20:6749–6754.

Onishi, H., S. Kojima, K. Katoh, K. Fujiwara, H. M. Martinez, and M. F. Morales. 1998. Functional transitions in myosin: formation of a critical salt-bridge and transmission of effect to the sensitive tryptophan. *Proc. Natl. Acad. Sci. U.S.A.* 95:6653–6658.

Onishi, H., K. Konishi, K. Fujiwara, K. Hayakawa, M. Tanokura, H. M. Martinez, and M. F. Morales. 2000. On the tryptophan residue of smooth muscle myosin that responds to binding of nucleotide. *Proc. Natl. Acad. Sci. U.S.A.* 97:11203–11208.

Park, S., K. Ajtai, and T. P. Burghardt. 1996. Cleft containing reactive thiol of myosin closes during ATP hydrolysis. *Biochim. Biophys. Acta.* 1296: 1–4.

Park, S., and T. P. Burghardt. 2000. Isolating and localizing ATP-sensitive tryptophan emission in skeletal myosin subfragment 1. *Biochemistry.* 39:11732–11741.

Peyser, Y. M., K. Ajtai, T. P. Burghardt, and A. Muhlrad. 1999. Characterization of myosin–ADP–phosphate analog complexes by trinitrophenylation of Lys^{83}. *J. Muscle Res. Cell Motil.* 20:814.

Peyser, Y. M., K. Ajtai, M. M. Werber, T. P. Burghardt, and A. Muhlrad. 1997. Effect of metal cations on the conformation of myosin subfragment-1–ADP–phosphate analog complexes: a near UV circular dichroism study. *Biochemistry.* 36:5170–5178.

Peyser, Y. M., M. Ben-Hur, M. M. Werber, and A. Muhlrad. 1996. Effect of divalent cations on the formation and stability of myosin subfragment 1–ADP–phosphate analog complexes. *Biochemistry.* 35:4409–4416.

Phan, B., and E. Reisler. 1992. Inhibition of myosin ATPase by beryllium fluoride. *Biochemistry.* 31:4787–4793.

Phan, B. C., Y. M. Peyser, E. Reisler, and A. Muhlrad. 1997. Effect of complexes of ADP and phosphate analogs on the conformation of the Cys^{707}–Cys^{697} region of myosin subfragment 1. *Eur. J. Biochem.* 243: 636–642.

Smith, C. A., and I. Rayment. 1996. X-ray structure of the magnesium(II)–ADP–vanadate complex of the *Dictyostelium discoideum* myosin motor domain to 1.9 Å resolution. *Biochemistry.* 35: 5404–5417.

Strickland, E. H. 1974. Aromatic contributions to circular dichroism spectra of proteins. *Crit. Rev. Biochem.* 113–175.

Tonomura, Y., P. Appel, and M. F. Morales. 1966. On the molecular weight of myosin. II. *Biochemistry.* 5:515–521.

Tonomura, Y., J. Yoshimura, and T. Onishi. 1963. On the active site of myosin A-adenosine triphosphatase. IV. Properties of binding of trinitrobenzenesulfonate and P-chloromercuribenzoate to myosin A. *Biochim. Biophys. Acta.* 78:698–700.

Von Hippel, P. H., and K. Y. Wong. 1964. Neutral salts: the generality of their effects on the stability of macromolecular conformations. *Science.* 145:577–580.

Weeds, A. G., and R. S. Taylor. 1975. Separation of subfragment-1 isoenzymes from rabbit skeletal muscle myosin. *Nature.* 257:54–56.

Werber, M. M., Y. M. Peyser, and A. Muhlrad. 1992. Characterization of stable beryllium fluoride, aluminum fluoride, and vanadate containing myosin subfragment 1-nucleotide complexes. *Biochemistry.* 31: 7190–7197.

Werber, M. M., A. G. Szent-Györgyi, and G. D. Fasman. 1972. Fluorescence studies on heavy meromyosin–substrate interaction. *Biochemistry.* 11:2872–2883.

Yengo, C. M., L. R. Chrin, A. S. Rovner, and C. L. Berger. 2000. Tryptophan 512 is sensitive to conformational changes in the rigid relay loop of smooth muscle myosin during the MgATPase cycle. *J. Biol. Chem.* 275:25481–25487.

Yount, R. G. 1997. Myosin as a motor and a back door enzyme. *FASEB J.* 11:A855.